Proceedings of ICFDP9:
Ninth International Congress of Fluid Dynamics & Propulsion
December 18-21, 2008, Alexandria, Egypt

ICFDP9-EG-219

Effect of A Tuned Liquid Damper Screen Configuration on Structure Response

H.Morsy **M. Marivani** **M. S. Hamed**

ABSTRACT

The dynamic response of a single-degree of freedom (SDOF) structure equipped with a TLD that has a slat screen was investigated. Liquid sloshing motion under external excitations was simulated using an in-house numerical model. The numerical algorithm is an integrated fluid-structure model that reconstructs the moving fluid surface using the "Volume of Fluid" method and resolves flow through the screen using the "Partial-cell treatment" method. The algorithm was validated against experimental data for cases of TLD with and without a slat screen. The initial data findings showed an expected 72% reduction in structural deflection when TLDs with a screen was used. A series of test cases with screens that have different solidities were carried out and an added increase of up to 32% was recorded in building deflection.

NOMENCLATURE:

A	Amplitude of external dynamic excitation, m
g_i	Gravitational acceleration, m/s^2
L	Length of tank, m
d	Height of the initial flat free surface, m
p	Pressure, Pa
t	Time, s
u,v	Velocity components in the horizontal and vertical directions, respectively
x,y	Cartesian coordinates
F	Volume of fluid per unit volume of cell (I,J)
F_e	External excitation force, N
D	Tank horizontal Displacement
D_s	Slat Height
S	Solidity ratio
S_s	Total Solid Height of Screen
P	Total momentum of fluid, kg.m/s
M_s	Mass of Structure, kg
C_s	Generalized damping of Structure, N.s/m
K_s	Stiffness of Structure, N/m
X_s	Displacement of Structure, m
T	Period of Sloshing, sec
F_{TLD}	Sloshing force, N
f_{TLD}	Natural frequency of TLD, hz

GREEK:

μ	Dynamic viscosity, m^2/s
σ	Stress tensor, N/m^2
θ	Partial flow flag
φ	Phase angle, deg

ω	Frequency of sloshing
ξ	Damping ratio
β	Ratio of excitation frequency to natural frequency
ρ	Density, kg/m^3
τ	Shear stress, N/m^2

KEYWORDS:
Tuned liquid dampers, TLD, Vibration Absorber, Sloshing, Screens, Dynamic Vibration Absorber.

INTRODUCTION

Tuned liquid dampers (TLDs) are partially filled water tanks that are used to mitigate vibration and motion in numerous engineering applications, most recently being civil structures. The tendency towards leaner and taller buildings, make the highly economic and simple TLDs the center of focus in a lot of research activities looking to protect structures from earthquake and wind force excitations. The addition of slat screens in TLDs introduces more linear behavior to the fluid sloshing motion and higher damping ratios.

The term "Tuned" refers to the fact that TLDs are designed to have a natural frequency equal to the natural frequency of the structure. This ensures that when excitation causes the sloshing motion of fluid inside the tank, the inertia forces created would be approximately anti-phase to the building motion (Lamb 1932). The first attempt at coupling a TLD to civil engineering structures was initiated by Bauer (1984), and further investigated by Kareem and Sun (1987).

There are a number of important design parameters that have to be considered when studying TLDs. Mass ratio is the mass of the sloshing fluid to the mass of the structure to be damped. All studies as early as the eighties until now have confirmed that this ratio is directly proportional to TLD efficiency in mitigating the vibration excitation (Ju et al, 2004). The limiting factor in this parameter is the available space on top of the civil structure to install the TLD. Another parameter is the damping ratio, which is defined as the ratio of the damping imposed by the TLD to the critical damping. This parameter provides a mathematical means of expressing the level of damping in a system (Warburton, 1982).

TLDs can be classified into shallow-water or deep-water TLDs depending on the Fluid Height to Tank Length Ratio (d/L). Deep-water TLDs (d/L>0.1) were investigated and found to have insufficient damping values to impose proper vibration suppression (Sun 1991). On the other hand, Shallow-water TLDs have desirable high values of damping, due to the fact that they tend to experience wave breaking under excitation, which results in damping ratios that can be an order of magnitude higher than damping ratios experienced in deep-water TLDs. However, their impracticality arises from the extreme nonlinearity and unpredictability of wave breaking. Due to its low (d/L) value, shallow-water TLDs have a non-desirable low value of mass ratio.

As a result there were numerous research efforts exerted to design additional damping devices to be added on deep-water TLDs [1, 3, and 4]. This study investigates the response of a structure rigidly coupled with a TLD equipped with a screen (See figure 4). The numerical algorithm used is an in-house developed code that can handle any type of TLD under a wide range of exciting amplitudes and frequencies. It also fully resolves the flow through the screen, rather than model it as a point hydraulic resistance like previous models. The mathematical formulation of the numerical algorithm will be discussed in the next section. The second section will present data that validates the algorithm against experimental investigations carried out by Tait et al (2004, 2005). After that, results of the dynamic response of a single degree of freedom (SDOF) structure equipped with a TLD with and without a screen are presented and discussed. The effect of the screen solidity is then tested and the results of the optimal screen configuration are reported.

2. Numerical Study Development

2.1 Governing Equations and Boundary Conditions

This study uses a one-phase approach in solving the Navier-Stokes equations, despite the fact that a gas phase exists in cells containing the interface separating the liquid surface and the above gas. This approach solves the momentum equation only in the liquid phase, and the effect of the gas is taken into account as a pressure boundary condition. Overall, the one phase approach is computationally less expensive than using a two-phase approach and the gas behavior above the free surface is of no importance in this application.

Two dimensional, incompressible free surface fluid flow is modeled in an Eulerian frame. Fixed points $\mathbf{x}$ in the domain ($\mathbf{x} = x\hat{i} + y\hat{j}$) are described using Cartesian coordinate. The velocity field $\mathbf{V}$ depends upon space and time:

$$\mathbf{V} = u(x,y,t)\hat{i} + v(x,y,t)\hat{j}$$

The governing equations of the incompressible, Newtonian, laminar flow in the Cartesian coordinate system are the following continuity and momentum equations:

$$\frac{\partial u}{\partial x} + \frac{\partial v}{\partial y} = 0 \qquad (1)$$

$$\frac{\partial u}{\partial t} + u\frac{\partial u}{\partial x} + v\frac{\partial u}{\partial y} = -\frac{1}{\rho}\frac{\partial p}{\partial x} + g_x + \frac{1}{\rho}\frac{\partial \tau_{xx}}{\partial x} + \frac{1}{\rho}\frac{\partial \tau_{xy}}{\partial x} \qquad (2)$$

$$\frac{\partial v}{\partial t} + u\frac{\partial v}{\partial x} + v\frac{\partial v}{\partial y} = -\frac{1}{\rho}\frac{\partial p}{\partial y} + g_y + \frac{1}{\rho}\frac{\partial \tau_{yy}}{\partial y} + \frac{1}{\rho}\frac{\partial \tau_{xy}}{\partial y} \quad (3)$$

Equations 1-2 are subject to the following set of boundary conditions.

-Viscous velocity boundary conditions at rigid walls are enforced by no-slip velocity boundary condition, i.e., zero tangential velocity over walls.

-The vertical component of the velocity on the walls is enforced to be zero due to non-penetrating wall boundary condition.

-On the free surface, the continuity of stress components which is referred to as dynamic boundary conditions must be satisfied. Since at free surface, viscous effects are neglected, the continuity of tangential stress components are satisfied automatically. Assuming small curvature of free surface in our interested applications simplifies the continuity of normal stress components as: $p_S = 0.0$ where p_S is the free surface pressure.

-Kinematics boundary condition must also be satisfied at free surface. This boundary condition assumes the velocity continuity at free surface in order to ensure the conservation of mass.

2.2 Volume of Fluid Method

The time evolution of the liquid region is computed by solving the following equation,

$$\frac{DF}{Dt} = 0 \quad (4)$$

where F is the local volume fraction of the liquid.

In the discretized sense, F is unity in computational cells occupied with liquid, and in cells occupied with gas, F is zero. For cells containing the interface bounding the liquid and gas phases, F lies between zero and unity. For these cells a donor-acceptor method is used, where at each boundary of each computing cell the two cells immediately adjacent to the interface are distinguished; one becoming a donor cell and the other an acceptor cell. Cell quantities are then given the subscripts D and A, respectively. The labeling is accomplished based on the algebraic sign of the fluid velocity normal to the boundary. Then the volume of fluid flux is calculated by a geometrical analysis using the free surface profile in the previous time step and the velocity field in the new time step. The new advanced F values are determined using the calculated volume of fluid flux at each cell face. The boundary slope and the side occupied by the liquid are determined using the gradient of F which represents the normal vector to the free surface.

Once the boundary slope and the side occupied by the liquid have been determined, a line can be constructed in the cell with the correct amount of F volume lying on the fluid side. This line is used as an approximation to the actual boundary and provides the information necessary to calculate the fluid height for the application of free surface pressure boundary conditions.

2.3 Partial Cell Treatment Method

The present model uses the partial cell treatment method to fully resolve the flow through the screen. In this method, internal obstacles are modeled as a special case of two phase flow in which the first phase is the fluid, with volume fraction θ , and the second phase is the obstacle with a fraction value of (1- θ). The obstacle is characterized as a fluid of infinite density and zero velocity. The continuity and momentum equations thus are modified to be:

$$\nabla.(\theta \quad \vec{u}) = 0 \quad (5)$$

and

$$\frac{\partial(\theta.\vec{u})}{\partial t} + \nabla.(\theta\vec{u}\vec{u}) = \theta\left[\vec{g} - \frac{\vec{\nabla}p}{\rho}\right] + \nabla.\left(\frac{\theta\vec{\vec{\sigma}}}{\rho}\right) \quad (6)$$

When the two-phase flow equations of motion are specialized to these conditions, they yield:

$$\frac{\partial(\theta.u_i)}{\partial x_i} = 0.0 \quad (7)$$

$$\frac{\partial(\theta.u_i)}{\partial t} + \theta.u_j\frac{\partial(\theta.u_i)}{\partial x_j} = -\frac{\theta}{\rho}\frac{\partial p}{\partial x_i} + \theta.g_i + \theta\frac{\partial}{\partial x_j}\left[2\upsilon\sigma_{ij}\right] \quad (8)$$

2.4 Algorithm Flowchart

To satisfy the continuity equation, pressures and velocities must be adjusted in each mesh cell. For cells that contain liquid only, the momentum equation is used to produce provisional velocity field. This is used with the continuity equation to obtain a pressure correction. This process is iterated until convergence, and the updated velocity and pressure fields are taken as the advanced time values. For cells that contain free surface, the cell pressure is obtained by interpolation between surface pressure and pressure for a neighboring cell containing fluid only. The iteration process also occurs here using pressure correction values from the liquid occupied cells. After the velocity and pressure fields have been obtained for a fixed F-field, F is advanced in time, using the donor and acceptor algorithm. New values of F are used to determine the slope and location of free surface in each cell boundary (See Figure 1).

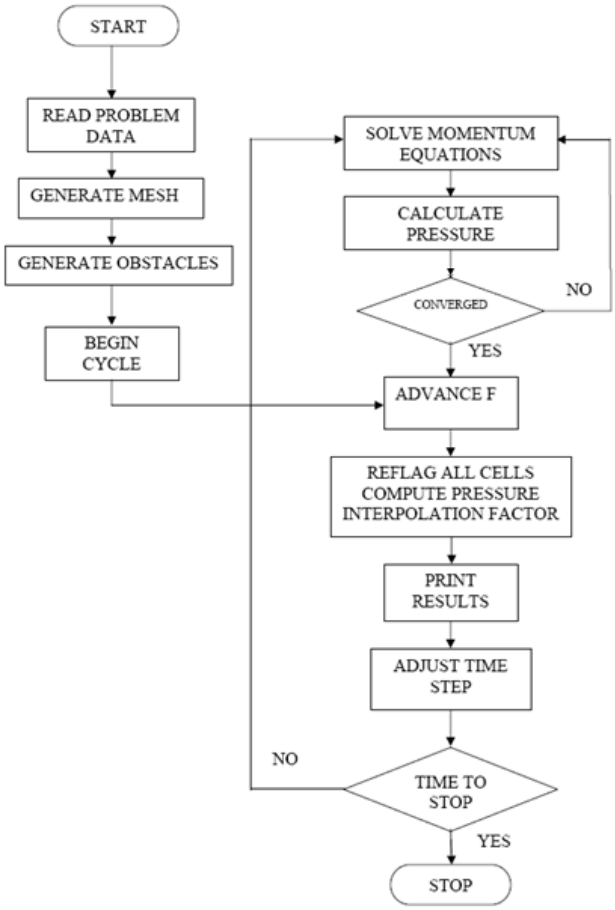

Figure 1 Algorithm Flowchart

2.6 Fluid – Structure Interaction Model

The Civil structure to be damped is modeled as a Single Degree Of Freedom (SDOF) body, with a mass M_s, Stiffness K_s, and damping coefficient C_s for simplicity. The TLD is mounted on top of the structure where maximum sway occurs.

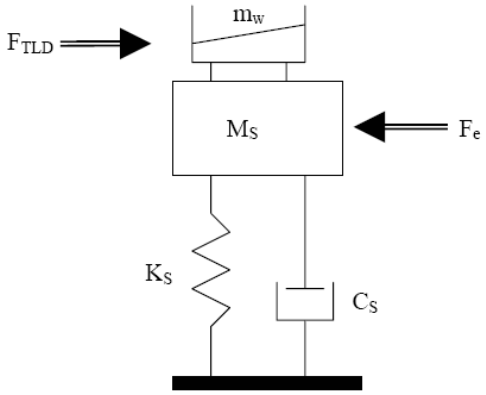

Figure 2 SDOF Coupled to a TLD

Figure 2 shows the coupled system under external excitation F_e. The TLD reacts with a sloshing force F_{TLD} supposedly anti-phase to the excitation force, and thus creates a damping effect that mitigates the swaying motion. The equation of motion of the coupled system is expressed as:

$$M_S \ddot{X}_S + C_S \dot{X}_S + K_S X_S = F_e + F_{TLD} \qquad (9)$$

In each computational cell the mass and velocity are calculated to predict the momentum value (P). This value is summed up for all computational cells to arrive at an estimate of the momentum for the sloshing fluid. The damping force F_{TLD} can then be determined by the following equation:

$$F_{TLD} = \frac{dP}{dt} \qquad (10)$$

Duhamel integral method has been used to solve the motion equation of the structure. The total displacement of a SDOF system exposed to an arbitrary external force $F(\tau)$ is given by:

$$X(t) = X_0 \cos \omega t + \frac{u_0}{\omega} \sin \omega t + \frac{1}{M\omega} \int_0^t F(\tau) \sin \omega (t-\tau) d\tau \qquad (11)$$

Setting initial displacement and velocity ($X_0, u_0 = 0$)results in:

$$X(t) = \frac{1}{M\omega_D} \int_0^t F(\tau) e^{-\xi\omega(t-\tau)} \sin \omega_D (t-\tau) d\tau \qquad (12)$$

where F is the sum of the external excitation force and the TLD sloshing force. Figure 3 presents the flow chart of the present overall numerical algorithm for the Fluid-Structure interaction model.

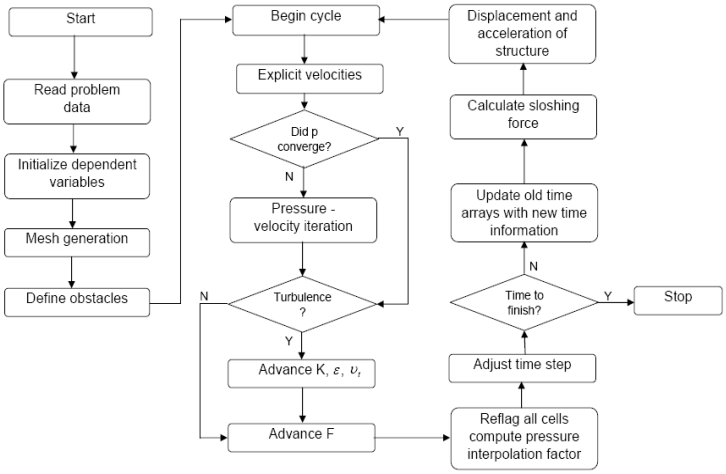

Figure 3 Flow chart of the overall Fluid-Structure interaction model

3. Validation: Sloshing of a Shallow Water Layer in a TLD with the slat screen

3.1 Experimental problem description

Since this study focuses on the case of a TLD with one screen, a similar experimental test case carried out by Tait et al [22,24] was considered. In this experimental study the TLD was subject to harmonic sinusoidal excitation. The tank was rectangular with Length (L)= 0.966 m, and the initial depth of water (d) was 0.119 m. The tank seen in Figure 4 was forced to move horizontally under the harmonic excitation. The displacement of the container is given by $D = A.Sin(\omega t + \phi)$.

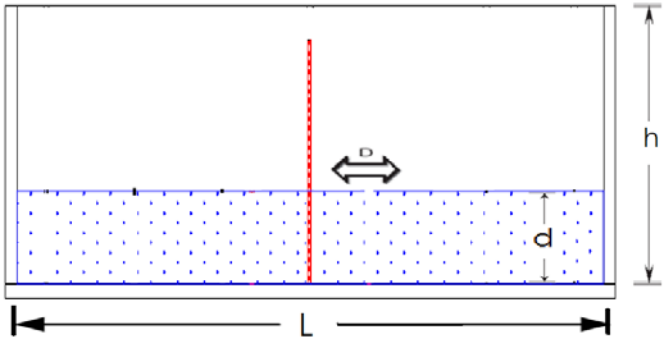

Figure 4. TLD Sketch

In this study the amplitude A, the period T, and the phase angle ϕ were 0.259 cm, 1.681s and 4.0, respectively. The screen was located in the middle of the tank and consisted of horizontal slats uniformly spaced apart. Screens are usually defined by their Solidity Ratio (S), which is defined as the ratio of the blocked area to the total area of the screen. For this study S was set to 0.5, so the width of each slat (D_s) was 5 mm with 5 mm spacing between each slat, and the thickness of each slat was 2.6 mm. Since the depth of fluid in the tank was 119 mm, the screen consisted of 12 slats in total.

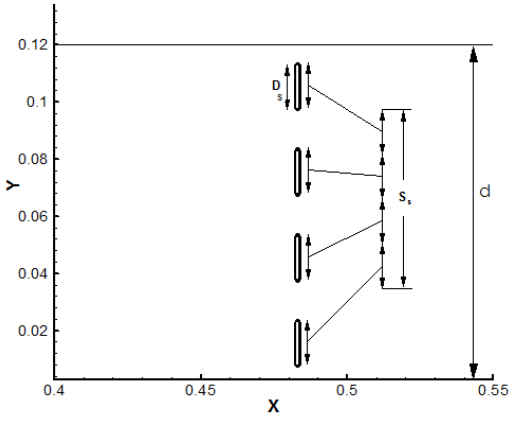

Figure 5. Screen Geometry showing slat heights and openings

The test case dimensions and exact loading values were modeled using the present in-house numerical algorithm. The grid throughout the TLD was checked for numerical dependency, and a final non-uniform grid of 260 x 200 grid points was finally used and gave acceptable results.

3.2 Comparison of Numerical & Experimental Results

In the experimental study, the free surface deflection was measured at a distance equal to 5% of tank length from the left side of the tank, and plotted against time. 2 cases were considered; one with a screen, and one without a screen. The numerical algorithm was tuned to generate the same parameter at the same location of the tank for both cases as well. Figure 6 shows the variation of this parameter for both cases with and without screen. The numerical results were in good agreement with the experimental data. As expected, using the screen eliminated the beating phenomena that appears in cases of low inherent damping, and resulted in a linear and controllable sloshing motion. Figure 7 shows a direct comparison of values for the experimental and numerical studies. A slight phase shift appeared between the experimental and the numerical results, because of a slight phase shift between the actual excitation used in the experiment and the one used in the numerical computations.

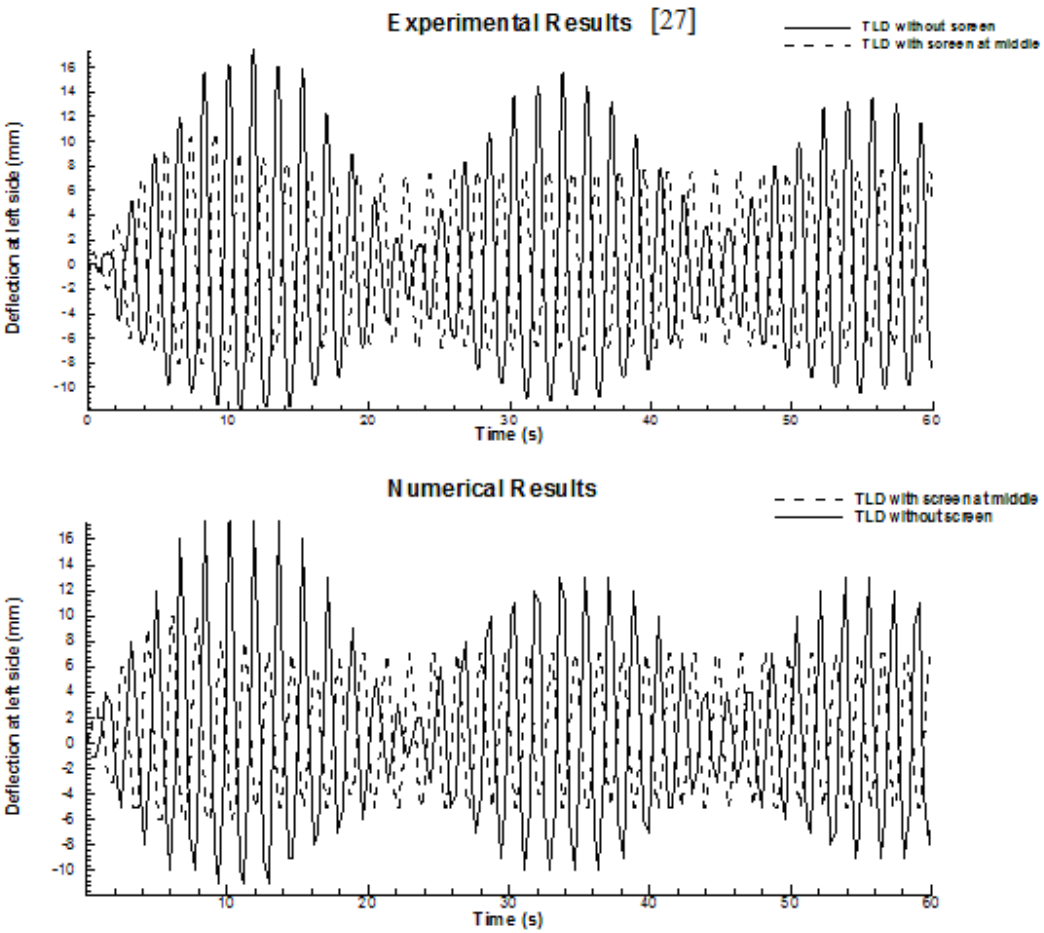

Figure 5: Surface deformations at a location 5% of tank length from the left wall

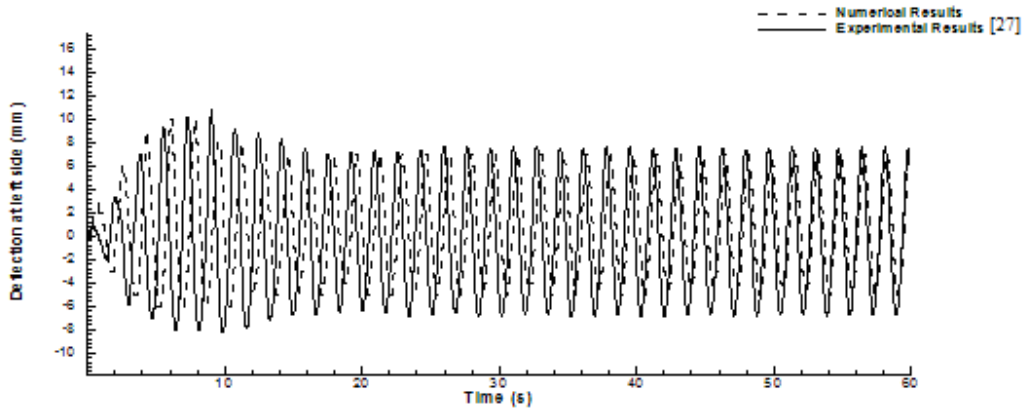

Figure 6: Surface deformations at a location 5% of tank length from the left wall with screen at the middle of tank

4. Numerical Test Cases

In this case study, numerical simulations were carried out to model the response of a SDOF structure. Figure 2 shows the schematic of the SDOF structure that resembles a high rise building. The TLD is typically installed on the rooftop of the building, as it usually serves as a water tank for fire emergencies. The Structure properties were chosen to be similar to an experimental test study carried out by Tait et al [23,24]. The properties of the structure and the TLD are listed in table 1. In real life situations the excitation on any civil structure could be wind excitation, where amplitudes involved are usually low in value. In high rise buildings, this kind of force would cause structural deflection mostly sensed by the top floors. In minor cases, the occupants of that floor feel nauseous with the vibration, but in major incidents the window panels were reported to fall off the building (John Hancock Tower, Boston, USA). The harmonic excitation chosen in all test cases was A/L= 0.2 % (Amplitude is usually non-dimensionalized using tank length as reference).

Table 1: Structure properties

M_S (Kg)	K_S (N/m)	ξ (%)	μ (%)
4480	55100	0.1	2.5

Table 2: TLD properties

L (m)	h (m)	d (m)	f_{TLD} (Hz)
0.966	0.3	0.119	0.545

4.1 Effect of TLD on Structure Response

This part of the study was carried out partially to validate the TLD-Structure numerical model results against the experimental results, and partially to confirm TLD and screen effect in structure response. Structure Deflection in meters was captured against time in three different cases:

- No TLD installed
- TLD without a screen installed
- TLD with a screen installed

4.2 Effect of screen solidity on Structure Response

This part of the study was carried out to investigate whether or not screen solidity had a significant effect on Structure Response. Three typical solidities of 0.4, 0.5, and 0.6 were used, and the structure deflection was captured in each case.

5. The Numerical Results

Figure 8 shows a value of up to 71 % reduction in the structure deflection using a TLD without a screen. Between the 20 and 40 second mark in the numerical run, the structure experiences its worst deflection values. In this region, installing a screen reduces the deflection with a value up to 21 % more (taking the maximum deflection in the case of TLD without screen as reference).

Figures 9, 10, and 11 show the structure deflection for cases of screen solidity 0.4, 0.5, and 0.6, respectively. To effectively compare on common grounds, the maximum deflection was captured in each case after the first 10 seconds of transient response (see Table 3).

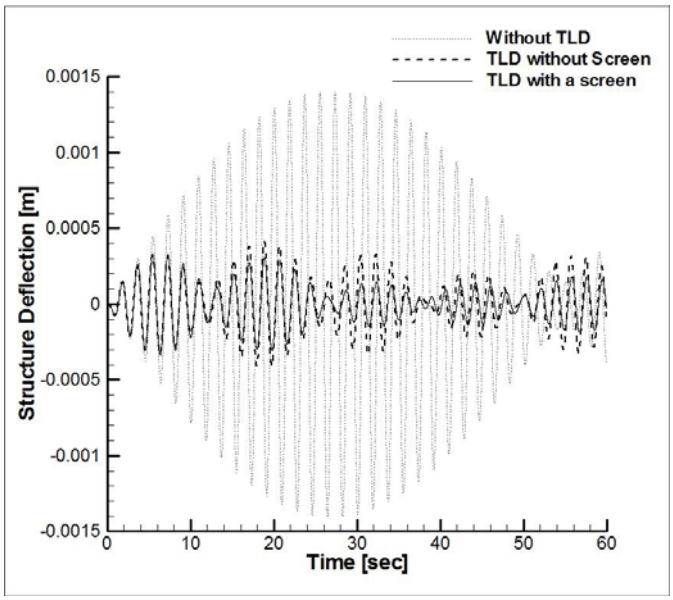

Figure 8: Structure Deflection comparison

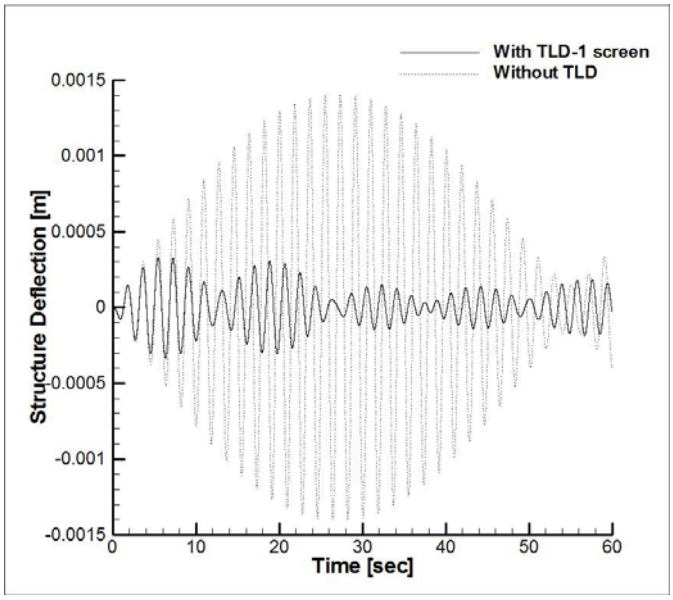

Figure 9: Structure Deflection for a TLD with a screen of S=0.4

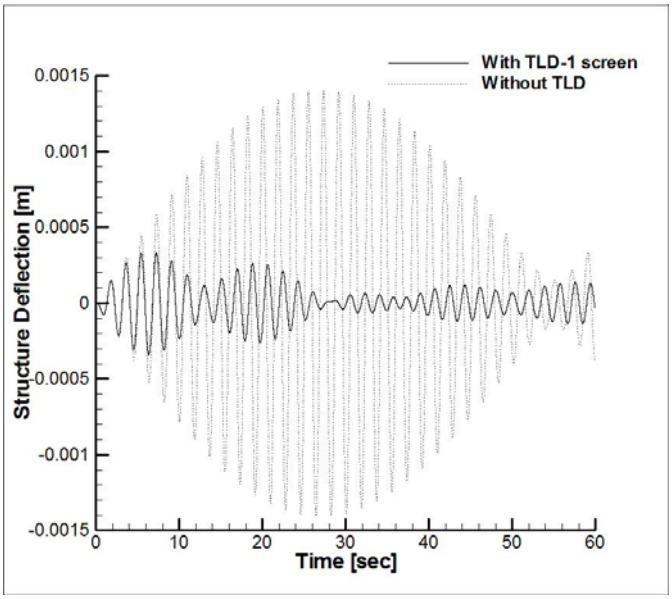

Figure 10: Structure Deflection for a TLD with a screen of S=0.5

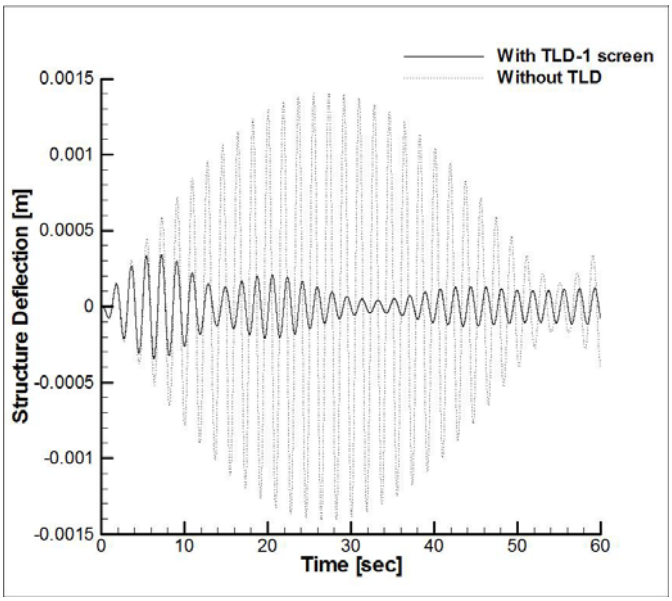

Figure 11: Structure Deflection for a TLD with a screen of S=0.6

Table 3: Maximum deflection for different solidities

Screen Solidity	Max. def. in [mm] after 10[sec]
0.4	0.3093
0.5	0.2617
0.6	0.2094

6. Conclusion

TLDs that are properly tuned to the building natural frequency have an extreme effect on structure response under harmonic excitation. Structure Deflection is decreased by up to 71 % even without using a screen. The introduction of a screen further increases TLD effectiveness through decreasing deflection by up to 21% more. The increase of the TLD screen solidity results in an expected increase in friction effect on the sloshing fluid through the screen, thus an increase in the damping ratio. If maximum structure deflection at S=0.4 is taken as a reference, then a change of solidity from 0.4 to 0.6 would lead to a 32.2 % further decrease in maximum structure deflection value. This increase in damping is also evident in the trend of the structure deflection plot in figures 8 through 11. Notice the beating phenomena is very obvious in figure 8 for the case of a TLD without a screen, and as the screen solidity is increased the beating phenomena fades away significantly.

REFERENCES

[1] Abramson, H. N. and Ransleben, G. E. (1961). "*Some Studies of a Floating Lid Type Device for Suppression of Liquid Sloshing in Rigid Cylindrical Tanks"*, Report TR-10, Contract DA-23-072- RD-1251, Southwest Research Institute.

[2] Banerji P., Murudi M., Shah. A.H. (2000). "Tuned Liquid Dampers for controlling earthquake response of structure", *earthquake eng Struct. Dyn.*, 29: 587-602

[3] Bauer, H. F. (1984). "Oscillations of Immiscible Liquids in a Rectangular Container a New Damper for Excited Structures", *Journal of Sound and Vibration*, 93(1), 117-133.

[4] Bauer, H. F. (1962). "*The Damping Factor Provided by Flat Annular Ring Baffles for Free Surface Oscillations"*, Report MTP-AERO-62-81, NASA-MSFC.

[5] Chopra (1980). "*Dynamics of structure: Theory and Application to Earthquake Engineering*", 1st Ed., Prentice Hall: NY, U.S.A

[6] Fediw, A.A., Isyumov, N., Vickery, B.J. (1995). "Performance of a tuned sloshing water damper", *Journal of Wind Engineering & Industrial Aerodynamics,* Vol. 57, pp. 237-247

[7] Hamed M.S. and Floryan J.M. (1998). "Numerical Simulation of Unsteady Nonisothermal Capillary Interfaces", *Journal of computational physics*, Vol.145, pp.110-140

[8] Hamelin J. (2007). "*The effect of screen geometry on the performance of a Tuned Liquid Damper*", MSc. Thesis, McMaster University

[9] Ju Y.K., Yoon S.W. and Kim S.D. (2004). "Experimental evaluation of a tuned liquid damper system", *Structures and Buildings*, Vol.157, issue 4, pp. 251-262

[10] Kaneko, S., Ishikawa, M. (1999). "Modeling of Tuned Liquid Damper With Submerged Nets", *Journal of Pressure Vessel Technology,* Vol. 121, pp. 334-341

[11] Kanok W. and Tam B.T. (1999). "Structure Fluid Interaction Model of Tuned Liquid Dampers", *Int. J. Numer. Methd. Eng*. 46. 1541-1558

[12] Kareem, A. and Sun, W.J. (1987). "Stochastic Response of Structures with Fluid Containing Appendages*", Journal of Sound and Vibration*, Vol. 119, No. 3, pp.389-408.

[13] Lamb, H. (1932). "*Hydrodnamics*", The University Press, Cambridge, England.

[14] Ransou S.R. and Hansen E.W. (2006), "Numerical simulations of sloshing in rectangular tanks", *Proceedings of OMAE2006 25th international conference on offshore mechanics and arctic engineering*, June 4-9, 2006, Hamburg, Germany

[15] Raad P. E, Johnson D. B., Chen S. (1994). "Simulation of Impacts of Fluid Free Surfaces with Solid Boundaries", *International Journal for Numerical Methods in Fluids*, Vol. 19, pp. 153-176.

[16] Reed, D., Jinkyu Y., Harry Y (1998). "Investigation of Tuned Liquid Dampers under Large Amplitude Excitation", *Journal of Engineering Mechanics,* ASCE, Vol. 124, No.4, pp. 405 -413

[17] Reed, D., Yu, J., Yeh, H. and Gardarsson, S. (1998). "Investigation of Tuned Liquid Dampers under Large Amplitude Excitation", *Journal of Wind Engineering and Industrial Aerodynamics,* Vol74-76, pp.923-930

[18] Siddique M.R., Hamed M.S., El Damatty A.A. (2004). "A nonlinear numerical model for sloshing motion in tuned liquid dampers", *International Journal for Numerical Methods in Heat & Fluid Flow,* Vol. 15 No. 3, pp. 306-324.

[19] Soong T.T. and Dargush G.F. (1997). "*Passive energy dissipation systems in structural engineering*", John Wiley.

[20] Sun L.M. (1991). "*Semi-Analytical Modeling of Tuned Liquid Damper (TLD) with Emphasis on Damping of Liquid Sloshing",* Ph.D. Thesis, University of Tokyo.

[21] Sun, L.M., Fujino, Y., Chaiseri, P. and Pacheco. (1995). "The Properties of Tuned Liquid Dampers using a TMD Analogy", *Earthquake Engineering and Structural Dynamics,* Vol. 24,pp. 967-976.

[22] Tait, M. (2004). "*The Performance of 1-D and 2-D tuned Liquid Dampers",* Ph.D. Thesis. University of Western Ontario, London, Canada.

[23] Tait, M., El Damatty, A.A., Isyumov, N. (2005). "An Investigation of tuned liquid dampers equipped with damping screens under 2D excitation", *Earthquake Engineering and Structural Dynamics,* Vol. 34, pp. 719-735.

[24] Tait, M., El Damatty, A.A., Isyumov, N. (2005). "Effectiveness of a 2D TLD and its numerical modeling", *Journal of structural engineering,* Vol. 34, pp. 79-96.

[25] Tait, M., El Damatty, A.A., Isyumov, N., Siddique, M.R. (2005). "Numerical Flow Models to Simulate Tuned Liquid Dampers (TLD) with Slat Screens", *Journal of Fluids and Structures,* Vol. 20, No. 8, pp. 1007-1023.

[26] Warburton, G.B. (1982). "Optimum Absorber Parameters for Various Combinations of Response and Excitation Parameters", *Earthquake Engineering and Structural Dynamics*, Vol. 10, pp. 381-401

[27] Wilcox David C. (2002). "*Turbulence Modeling for CFD*", Second edition.

[28] Yalla, S.K. (2001). "*Liquid Dampers for Mitigation of Structural Response: Theoretical Development and Experimental Validation"*, Ph.D. Thesis, University of Notre Dame, Indiana, U.S.A

[29] YU J.K. (1997). "*Nonlinear characteristics of Tuned Liquid Damper*", PhD thesis, University of Tokyo

[30] Zang, Y., Xue, S. and Kurita, S. (2000). "A boundary element method and spectral analysis model for small-amplitude viscous sloshing in couple with structural vibrations", *International Journal for Numerical Methods in Fluids,* Vol. 32, pp. 79-96.